Kufa Journal of Engineering
Vol. 10, No. 1, January 2019, P.P. 92-110
Received 7 January 2018, accepted 6 March 2018

NUMERICAL INVESTIGATION OF NATURAL FREQUENCIES FOR CLAMPED LONGITUDINAL COMPOSITE PLATES

Firas T. Al-Maliky[1]

[1] University of Alkafeel, Faculty of Technique Engineering, Iraq. Email: firas.almaliky@alkafeel.edu.iq ; firasthair@yahoo.com

http://dx.doi.org/10.30572/2018/kje/100108

ABSTRACT

In this paper, two finite element models were performed. The fiber and matrix represented as two different materials in the first plate, while the second showed as a composite plate. The boundary conditions included clamped the plates on four ends and the dimensions of the composite plates were changed in this study. The finite element was performed and ANSYS 16.1 was employed in modeling. By comparing the results between the frequency ratio and mode numbers for different plate thickness, the results showed that natural frequencies calculated by these two model thickness of the (length/width) ratio will be more uniform and the error will be small. The numerical equations that performed from this study used to investigate the natural frequencies for longitudinal clamped composite plate.

KEYWORDS: Modal analysis, composite plate, natural frequency, FEM

1. INTRODUCTION

Laminated composite plates are used as a main component in primary aerospace and aircraft structures and marine structures because of their properties. Properties such as high specific strength and stiffness, high fatigue and corrosion resistance have attracted researchers and companies to use them instead of conventional materials. In the last few decades, the use of composite materials has been increased significantly (Sharma and Mittal, 2010). Generally, composite materials consist of two (or more) phases. The first one has is the strongest phase which is call fiber. Fiber is used to reinforce the other phase which it is usually polymer. Depending on the application and manufacturing process, fiber can be continuous or discontinuous and longitudinal or randomly oriented in the matrix. The distributed fibers in the matrix are used to transfer the loads to fibers (Gay et al., 2003; William and David, 2010).

Because of the requirement of high performance, the resonance behavior of the laminated structures materials in aerospace structures have been studied by many researchers. For example, Leissa (Leissa, 1973) studied the vibration of plate with various geometries. Crawly, 1979 showed experimentally the natural frequency and mode shapes of aluminum plates and compared the results with finite element method.

Recently, finite element method have been employed in analyzing the engineering structure. For instance, Reddy, 1979 used the finite element method to study the free vibration of simply-supported plates. Han and Petyt, 1996 estimated the natural frequency of laminated rectangular plates by extending the p-version finite element method. Also, different boundary conditions are using to study the free vibration for rectangular plates by Hsu, 2003. Pandit et al., 2007 analyzed the free vibration of laminated composite rectangular plate using finite element method. Sang and Sang-Hyun, 2008 proposed new analysis of vibration for simply supported composite plates. Latheswary et al., 2004 investigated the free vibration analysis of laminated composite plates in linear and non-linear. Akavci, 2007 examined the analysis of free vibration for simply supported composite plates. Andrzej and Gawryluk, 2016 studied the modal analysis for three composite blades and the results of natural frequencies and mode shapes were compared with the modal analysis for the cantilever composite beam and the fixed rotor with one composite blade. The free vibration analysis of composite plates with various boundary conditions were discussed in several research using several mathematical techniques (Nayak, 2008; Alexander et al., 2012; Lopatin and Morozov, 2011).

In this project, two models are performed to calculate the natural frequencies of clamped longitudinal composite plates with different dimensions. ANSYS 16.1 was used in analyzing these two models. In the first model, perfect bonding between fibers and matrix was assumed. While, the equivalent mechanical properties of composite plate were taken into account. The effects of dimensions of composite plate, volume fractions and mechanical properties of the composite plates were studied in order to find the correction factor between the two models.

2. MATERIAL PROPERTIES AND VOLUME FRACTIONS

The mechanical properties of fiber and matrix that are used in this work are presented in Table 1.

Table 1. Fiber and Matrix Properties

No.	Property	Unit	Fiber	Matrix
1	E	Pascal.	3.79E+11	1.70E+09
2	G	Pascal.	1.55E+11	7.00E+08
3	ν	---	0.35	0.3
4	ρ	kg/m^3	1440	1250

The effective mechanical properties of the composite plates depend on mechanical properties of matrix and fiber. In order to calculate the equivalent mechanical properties, the following procedure can be used (Gay et al., 2003):

1. The total volume fraction and the matrix volume fraction: in this work , the fiber volume fraction changes from (10%) to (40%) by increasing the volume fraction by (5%) and according to the following equation, the matrix volume fraction can be calculated.

$$\forall_m = 1 - \forall_f \qquad 1$$

2. Density of composite plate was found by using rule of mixture:

$$\rho = \forall_m \rho_m + \forall_f \rho_f \qquad 2$$

3. The modulus of elasticity along the *direction of the fiber (*Eq. 3)

$$E_1 = \forall_m E_m + \forall_f E_f \qquad 3$$

4. The modulus of elasticity in the transverse direction to the fiber axis was calculated from Eq. 4,

$$E_2 = E_m \left[\frac{1}{(1-\forall_f) + \left(\frac{E_m}{E_f}\right)\forall_f} \right] \qquad 4$$

5. Shear modulus of composite was computed from Eq. 5,

$$G_2 = G_m \left[\frac{1}{(1-\forall_f) + \left(\frac{G_m}{G_f}\right)\forall_f} \right] \qquad 5$$

6. Poisson Ratio was determined from Eq. 6,

$$\nu_{12} = \forall_m \nu_m + \forall_f \nu_f \qquad 6$$

According to these steps, the equivalent mechanical and physical properties of composite plates for different fiber volume fractions can be listed in Table 2.

Table 2. The equivalent mechanical and physical properties of composite plates.

No.	Fiber Volume Fraction $\forall_f$	Matrix Volume Fraction $\forall_m$	Modulus of Elasticity $E_1(N/m^2)$	Modulus of Elasticity $E_2(N/m^2)$	Modulus of Rigidty $G_{12}(N/m^2)$	Poisson Ratio ν_{12}	Density $\rho(kg/m^3)$
1	0.1	0.9	3.94E+10	1.89E+09	7.77E+08	0.305	1269
2	0.15	0.85	5.83E+10	2E+09	8.23E+08	0.3075	1278.5
3	0.2	0.8	7.72E+10	2.12E+09	8.74E+08	0.31	1288
4	0.25	0.75	9.6E+10	2.26E+09	9.32E+08	0.3125	1297.5
5	0.3	0.7	115E+10	2.42E+09	9.98E+08	0.315	1307
6	0.35	0.65	134E+10	2.61E+09	107E+08	0.3175	1316.5
7	0.4	0.6	153E+10	2.82E+09	116E+08	0.32	1326

3. FIRST FINITE ELEMENT MODEL

In this model, the fibers and matrices were represented as two different materials which are connected to each other by physical bond. Therefore, the mechanical and physical properties of fiber and matrix are used instead of the equivalent mechanical and physical properties of composite plates. In this model, the element Layer 99 is used and the number of layers depend on the thickness of composite plate and generally the thickness of each element considered in this work does not exceed 1 mm. In order to calculate the dimensions of this model and according to fiber volume fraction, dimensions of plate (length , width and thickness) and cross section area of fiber, the number of fibers , the number of matrices and the width of matrices can be calculated using the following procedure:

1. Calculating the volume of composite plate and the volume of one fiber using the following equations:

$$V_T = L * W * t \qquad 7$$

$$V_f = \pi r^2 * L \qquad 8$$

2. Calculating the number of fiber (n) for any fiber volume fraction using the following equation and assuming that the distance between any two neighboring fibers is constant along the composite plate:

$$\forall_f = \frac{V_f}{V_T} = \frac{n*\pi r^2*L}{L*W*t} = \frac{n*\pi r^2}{W*t} \qquad 9$$

$$n = \frac{\forall_f * W * t}{\pi r^2} \qquad 10$$

3. As maintained previously, the volume fraction of fiber and the width of composite plate are given. Also, the center of fiber lies on the center of cross section area of composite plate (i.e. lies at (t/2)). Now the number ,dimensions and number of layers of matrices and the number of fibers can be calculated.

In this model, the size of element is one of the most important factor in order to get an accurate result. Therefore, the suitable size of element is found for each volume fraction.

4. SECOND FINITE ELEMENT MODEL

In this model, the composite plate is represented as one material with equivalent mechanical and physical properties calculated previously (see Table 2). The element Layer 99 is also used in this model and the thickness of each layer in this model does not exceed (1 mm) as shown in Fig. 1.

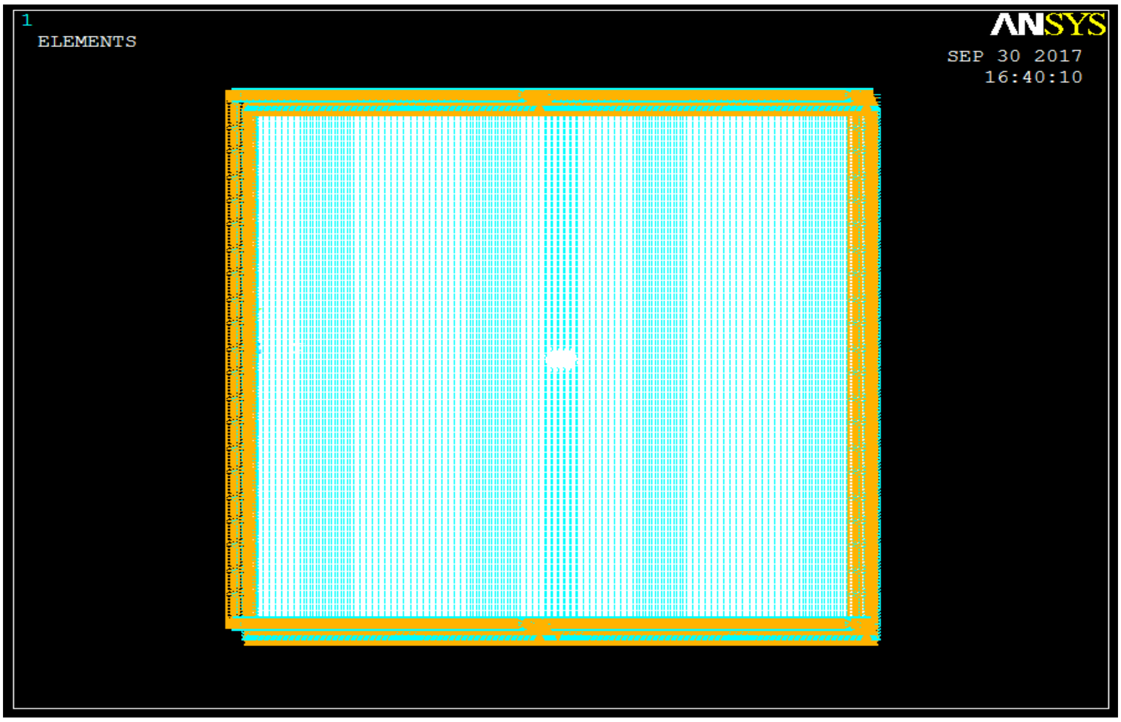

Fig. 1. Clamped longitudinal composite plates ($\forall_f = 0.25$ $\forall_m = 0.75$ with $L = 0.3 \times W = 0.3$ m and $t = 2$ mm).

5. DIMENSIONS AND BOUNDARY CONDITIONS OF COMPOSITE PLATE

The length and width of composite plates considered in this work are changed in order to study the effect of dimensions of plate on the natural frequency. On the other hand , the thickness of plate is changed and its values are (2 ,3 , 4 and 5) mm. These dimensions of plates can be summarized in Table 3. The clamped of the four ends of plates is the boundary condition used in this work.

Table 3. Dimensions of Composite Plates.

No.	Length (m)	Width (m)	Thickness (mm)
1.	0.1	0.1	2, 3, 4 and 5
2.	0.1	0.2	2, 3, 4 and 5
3.	0.1	0.3	2, 3, 4 and 5
4.	0.2	0.1	2, 3, 4 and 5
5.	0.2	0.2	2, 3, 4 and 5
6.	0.2	0.3	2, 3, 4 and 5
7.	0.3	0.1	2, 3, 4 and 5
8.	0.3	0.2	2, 3, 4 and 5
9.	0.3	0.3	2, 3, 4 and 5

6. RESULTS

In this work, several cases were studied including two finite element models of composite plates for different dimensions and thickness. Natural frequency ratio of the two models of composite plates can be predicted from Table 4. The results of natural frequencies that obtained from finite element analysis have been validated using ANSYS 16.1. Figs. 2, 4, 6 and 8 shows the comparison between the first, second, third, and fourth natural frequencies of the first model for different plate thickness due to changing in fiber volume fraction for different dimensions of plate using the first model while Figs. 3, 5, 7 and 9 shows the comparison between first, second, third, and fourth natural frequencies of the second model. The increasing in the thickness of composite plate increases the natural frequency with fixing the fiber volume fraction ratio, dimensions of composite plate and number of modes.

Fig. 10 represents the comparison between the frequency ratio due to changing in aspect ratio of plate (Length/ Width) for different plate thickness and mode numbers. It can be seen that the frequency ratio was increased proportionally with the increase in (Length/ Width) ratio for different plate thickness in the first, second, third and fourth mode respectively. Also, the relation between the natural frequencies calculating by these two model and the (length/width) ratio for first, second, third and fourth mode are shown in Figs. 11, 12, and 13. When the thickness of composite plate decreases, the relation between the natural frequencies calculating by these two model and the (length/width) ratio be more uniform and the error be small.

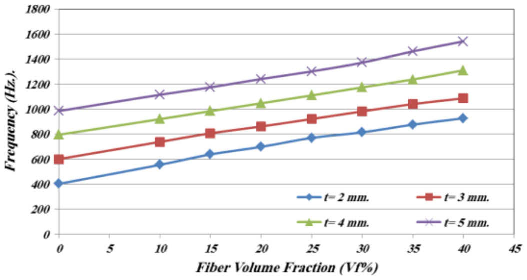

(a) L=0.1 m and W=0.1 m .

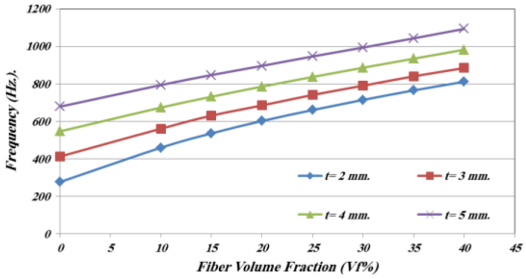

(b) L=0.1 m and W=0.2 m .

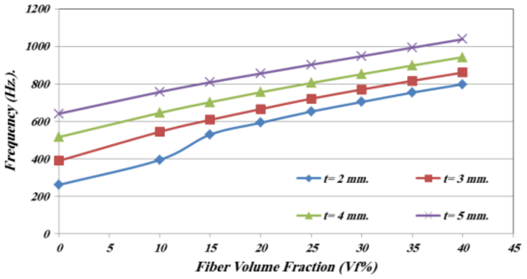

(c) L=0.1 m and W=0.3 m .

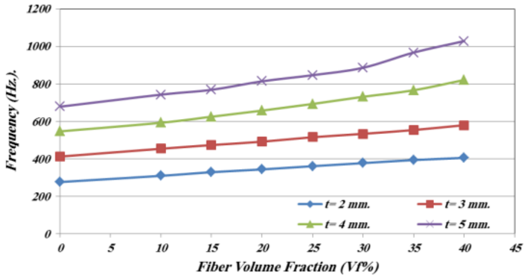

(d) L=0.2 m and W=0.1 m .

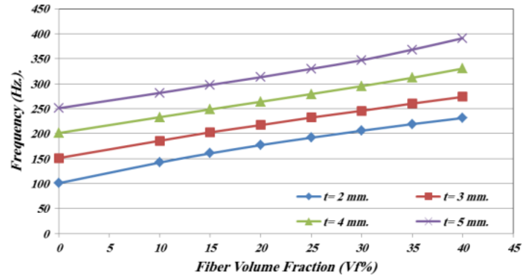

(e)L=0.2 m and W=0.2 m .

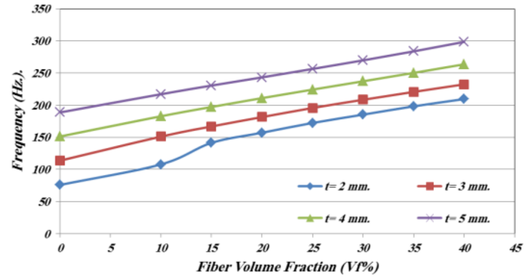

(f) L=0.2 m and W=0.3 m .

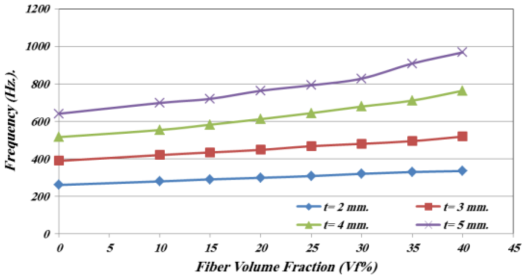

(g) L=0.3 m and W=0.1 m .

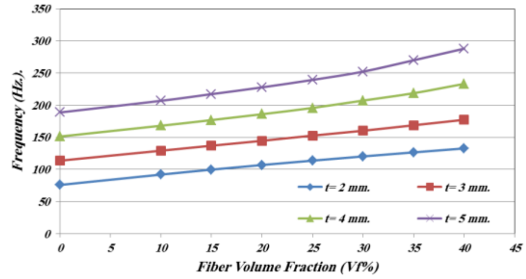

(h) L=0.3 m and W=0.2 m .

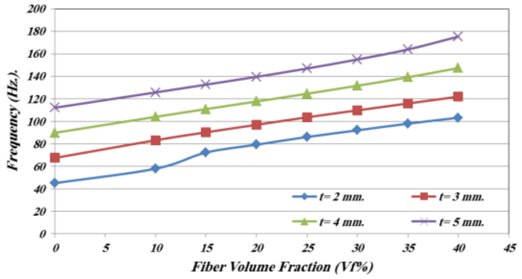

(i) L=0.3 m and W=0.3 m .

Fig. 2. Comparison Between the First Natural Frequencies for Different Plate Thickness Due to Change in Fibre Volume Fraction for Different Dimensions of Plate Using the First Model.

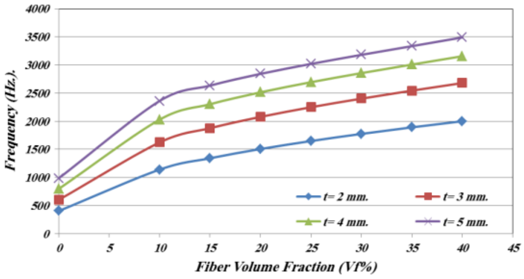

(a) L=0.1 m and W=0.1 m .

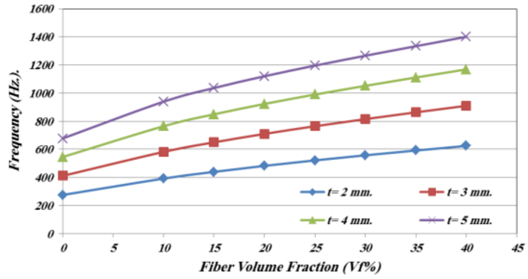

(b) L=0.1 m and W=0.2 m .

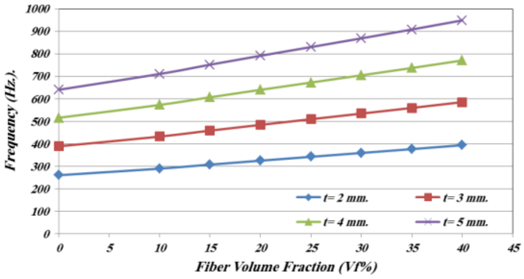

(c) L=0.1 m and W=0.3 m .

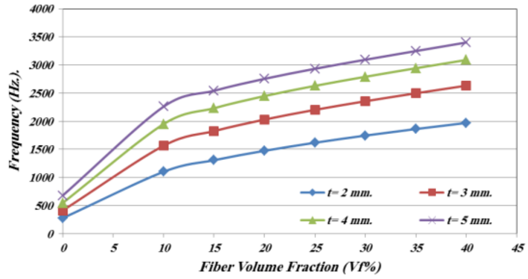

(d) L=0.2 m and W=0.1 m .

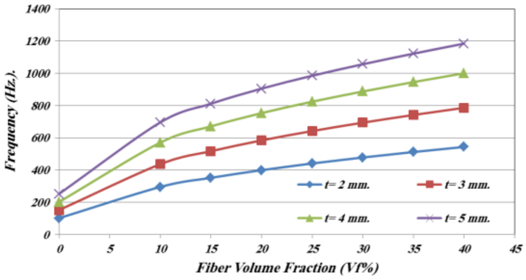

(e)L=0.2 m and W=0.2 m .

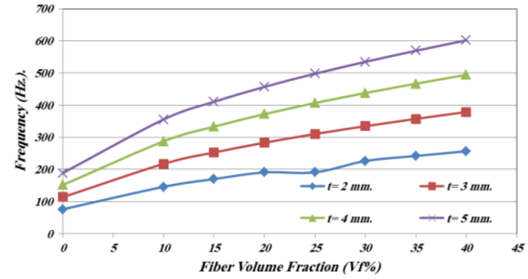

(f) L=0.2 m and W=0.3 m .

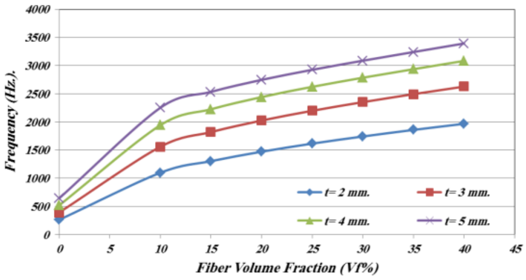

(g) L=0.3 m and W=0.1 m .

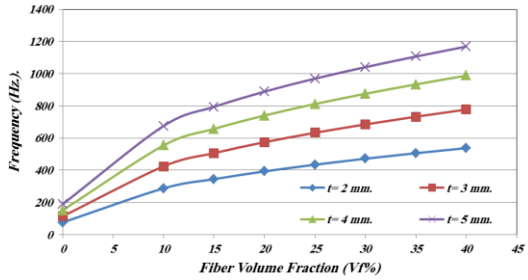

(h) L=0.3 m and W=0.2 m .

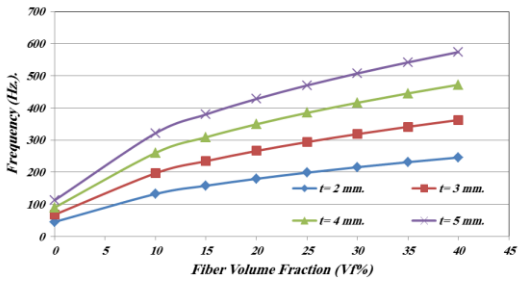

(i) L=0.3 m and W=0.3 m .

Fig. 3. Comparison Between the First Natural Frequencies for Different Plate Thickness Due to Change in Fibre Volume Fraction for Different Dimensions of Plate Using the Second Model.

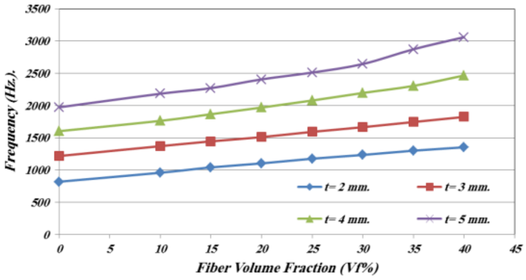

(c) L=0.1 m and W=0.1 m .

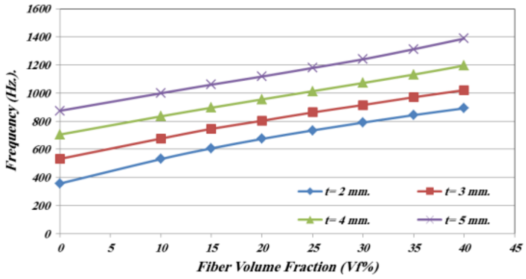

(d) L=0.1 m and W=0.2 m .

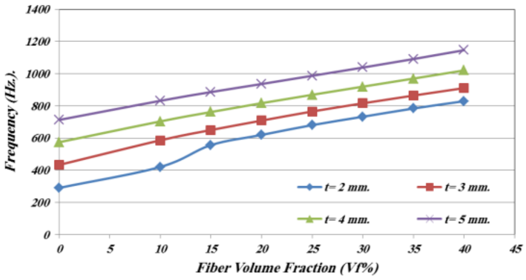

(c) L=0.1 m and W=0.3 m .

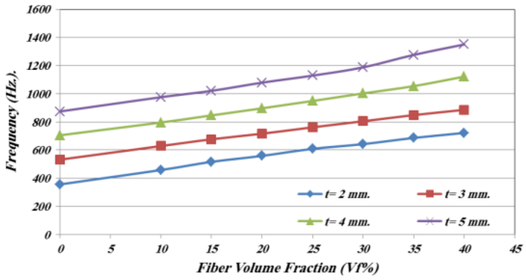

(d) L=0.2 m and W=0.1 m .

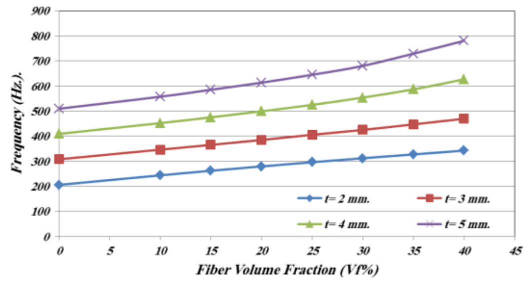

(e)L=0.2 m and W=0.2 m .

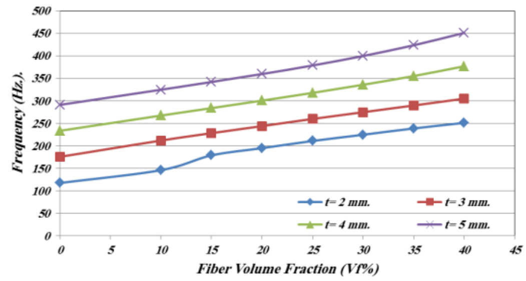

(f) L=0.2 m and W=0.3 m .

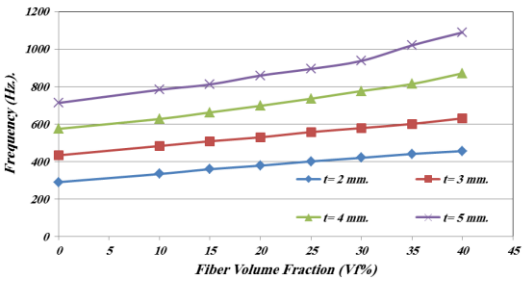

(g) L=0.3 m and W=0.1 m .

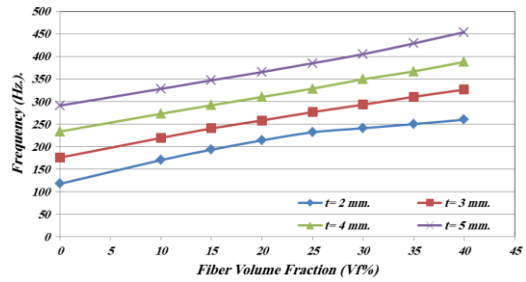

(h) L=0.3 m and W=0.2 m .

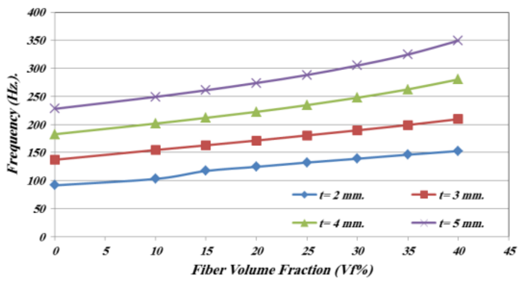

(i) L=0.3 m and W=0.3 m .

Fig. 4. Comparison Between the Second Natural Frequencies for Different Plate Thickness Due to Change in Fibre Volume Fraction for Different Dimensions of Plate Using the First Model.

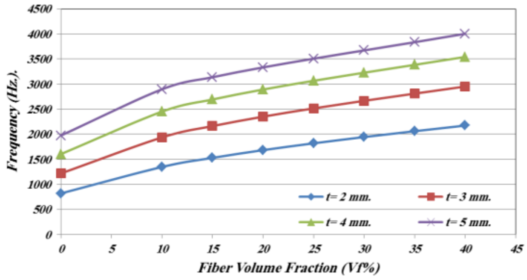

(a) L=0.1 m and W=0.1 m .

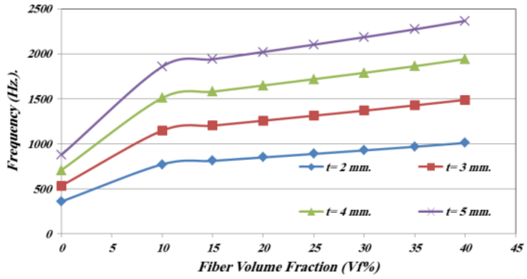

(b) L=0.1 m and W=0.2 m .

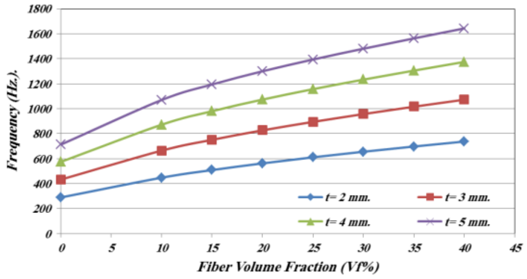

(c) L=0.1 m and W=0.3 m .

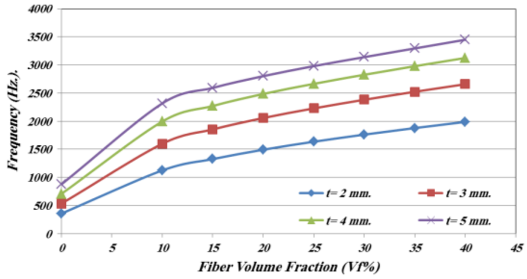

(d) L=0.2 m and W=0.1 m .

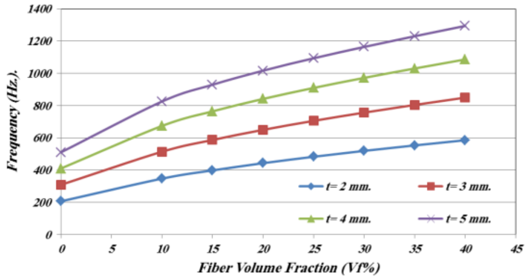

(e)L=0.2 m and W=0.2 m .

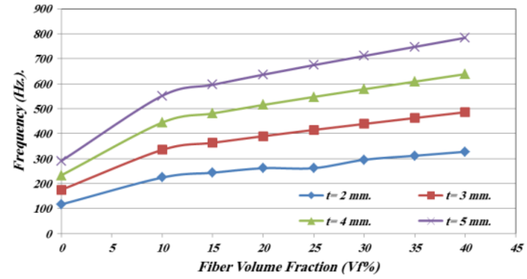

(f) L=0.2 m and W=0.3 m .

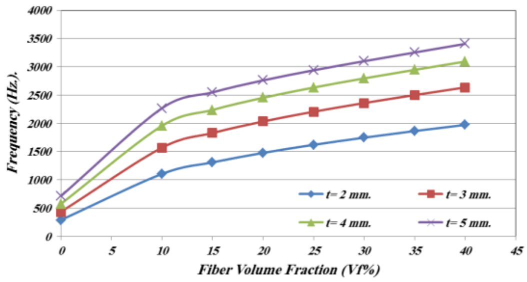

(g) L=0.3 m and W=0.1 m .

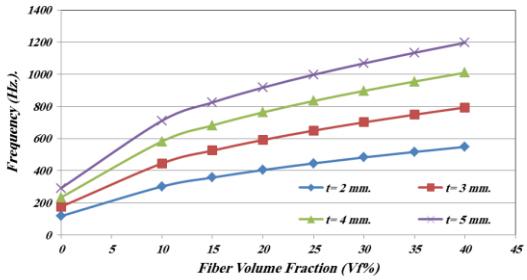

(h) L=0.3 m and W=0.2 m .

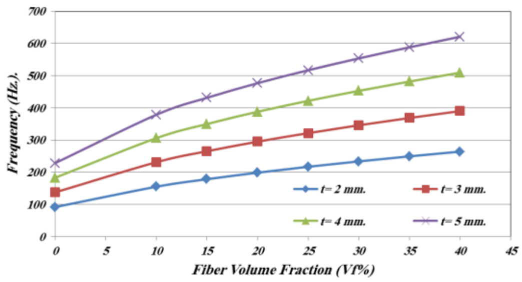

(i) L=0.3 m and W=0.3 m.

Fig. 5. Comparison Between the Second Natural Frequencies for Different Plate Thickness Due to Change in Fibre Volume Fraction for Different Dimensions of Plate Using the Second Model.

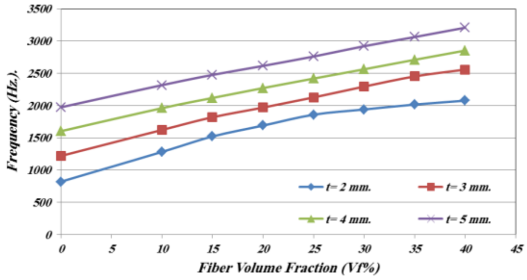

(a) L=0.1 m and W=0.1 m .

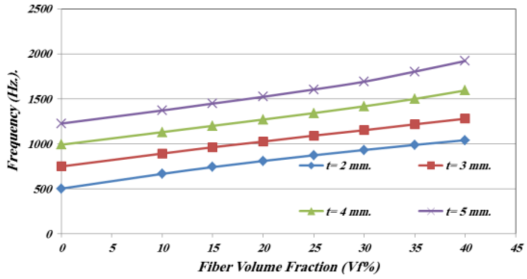

(b) L=0.1 m and W=0.2 m .

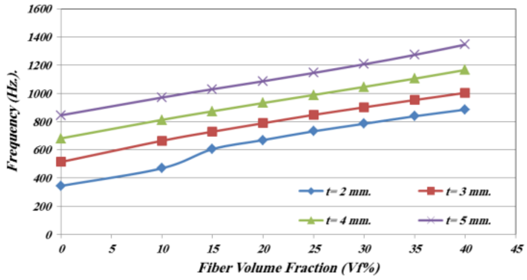

(c) L=0.1 m and W=0.3 m .

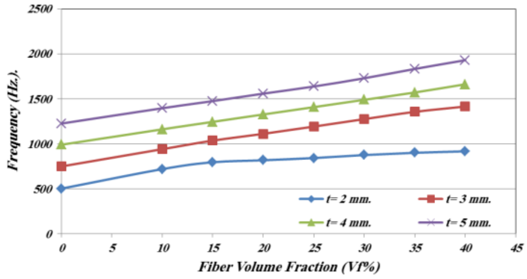

(d) L=0.2 m and W=0.1 m .

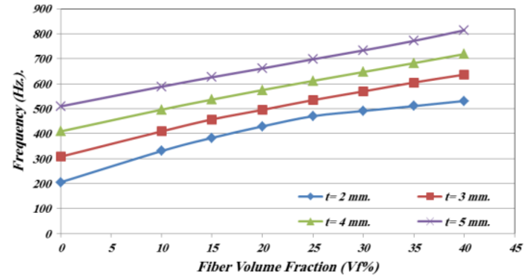

(e)L=0.2 m and W=0.2 m .

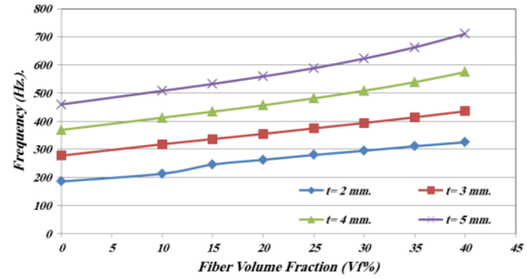

(f) L=0.2 m and W=0.3 m .

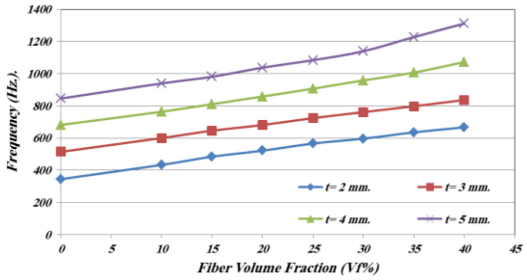

(g) L=0.3 m and W=0.1 m .

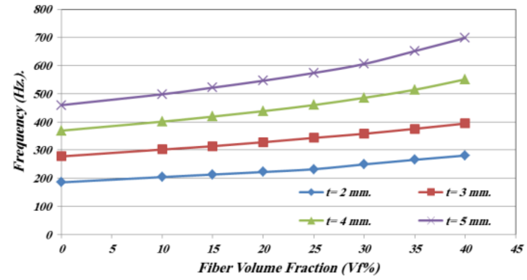

(h) L=0.3 m and W=0.2 m .

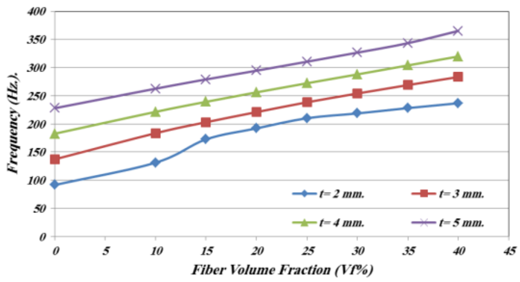

(i) L=0.3 m and W=0.3 m .

Fig. 6. Comparison Between the Third Natural Frequencies for Different Plate Thickness Due to Change in Fibre Volume Fraction for Different Dimensions of Plate Using the First Model.

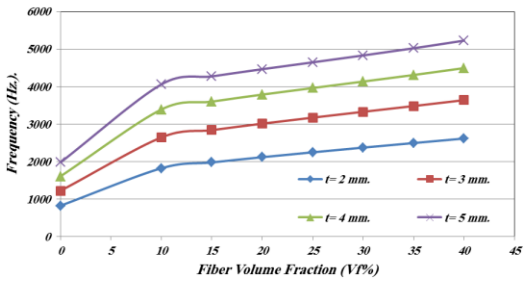

(a) L=0.1 m and W=0.1 m .

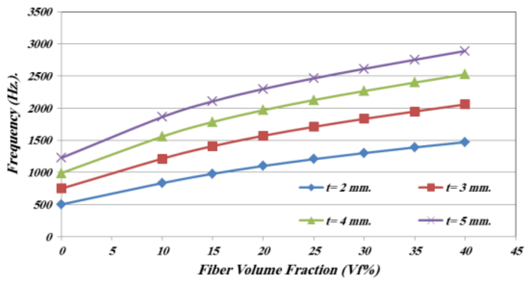

(b) L=0.1 m and W=0.2 m .

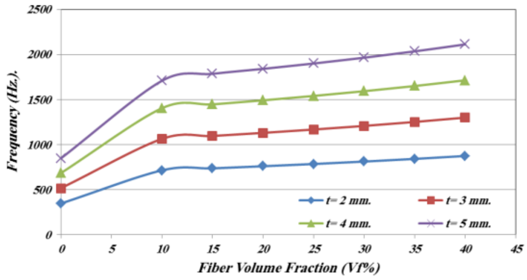

(c) L=0.1 m and W=0.3 m .

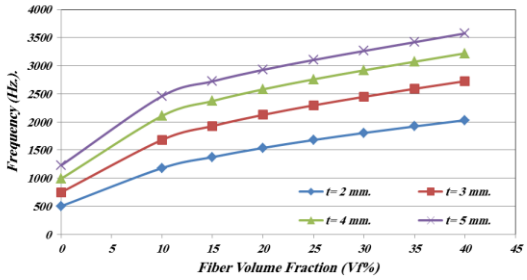

(d) L=0.2 m and W=0.1 m .

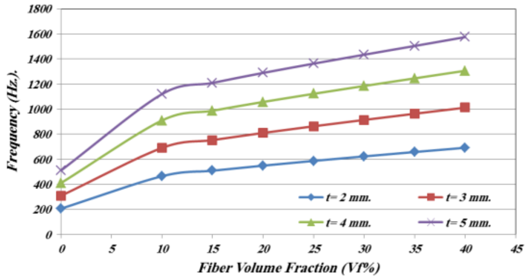

(e)L=0.2 m and W=0.2 m .

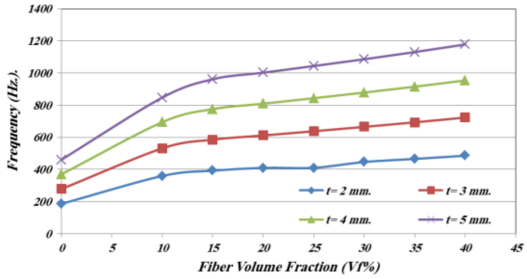

(f) L=0.2 m and W=0.3 m .

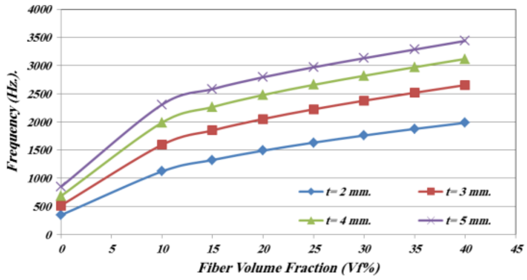

(g) L=0.3 m and W=0.1 m .

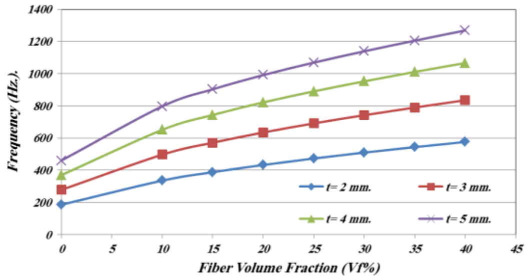

(h) L=0.3 m and W=0.2 m .

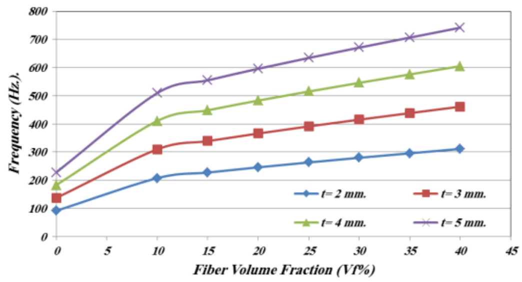

(i) L=0.3 m and W=0.3 m .

Fig. 7. Comparison Between the Third Natural Frequencies for Different Plate Thickness Due to Change in Fibre Volume Fraction for Different Dimensions of Plate Using the Second Model.

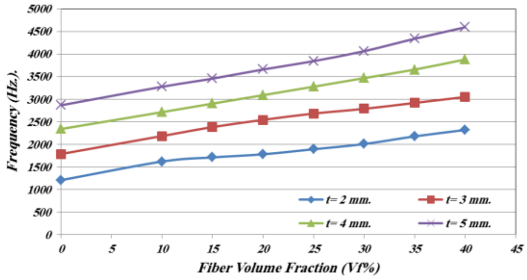

(a) L=0.1 m and W=0.1 m .

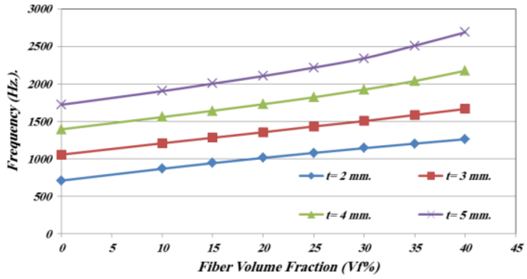

(b) L=0.1 m and W=0.2 m .

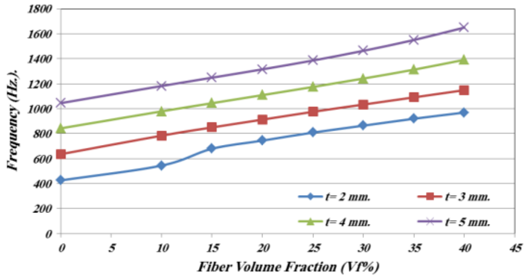

(c) L=0.1 m and W=0.3 m .

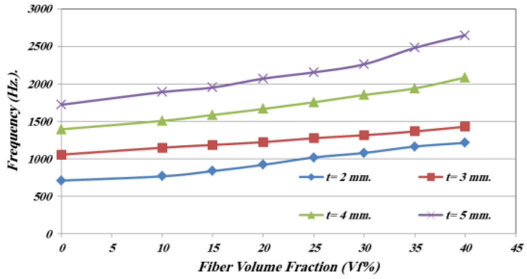

(d) L=0.2 m and W=0.1 m .

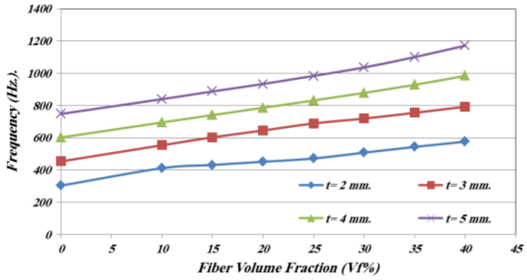

(e)L=0.2 m and W=0.2 m .

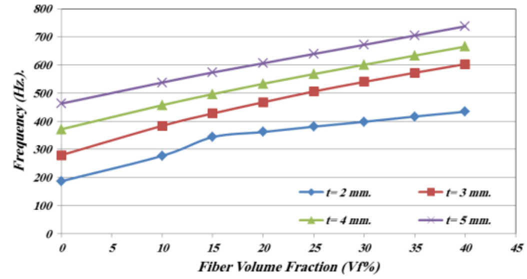

(f) L=0.2 m and W=0.3 m .

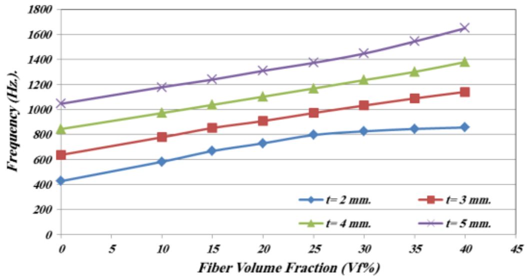

(g) L=0.3 m and W=0.1 m .

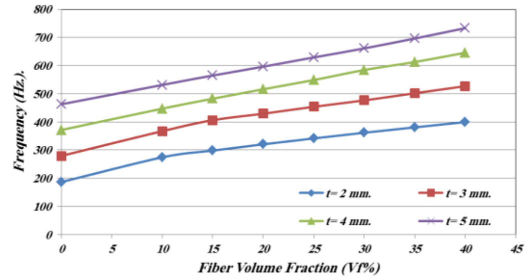

(h) L=0.3 m and W=0.2 m .

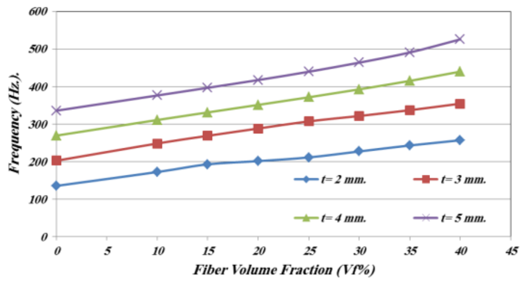

(i) L=0.3 m and W=0.3 m .

Fig. 8. Comparison Between the Forth Natural Frequencies for Different Plate Thickness Due to Change in Fibre Volume Fraction for Different Dimensions of Plate Using the First Model.

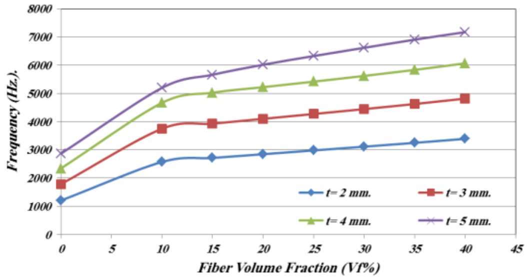

(a) L=0.1 m and W=0.1 m .

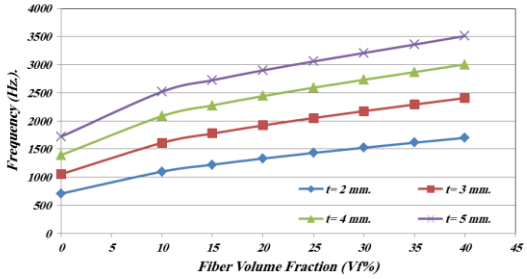

(b) L=0.1 m and W=0.2 m .

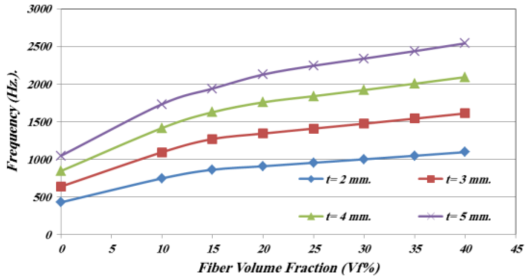

(c) L=0.1 m and W=0.3 m .

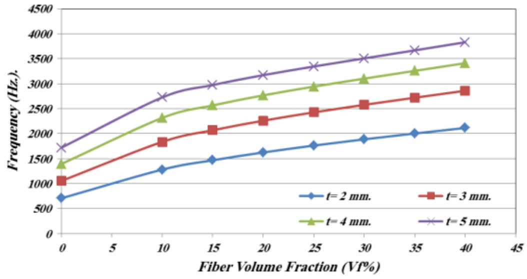

(d) L=0.2 m and W=0.1 m .

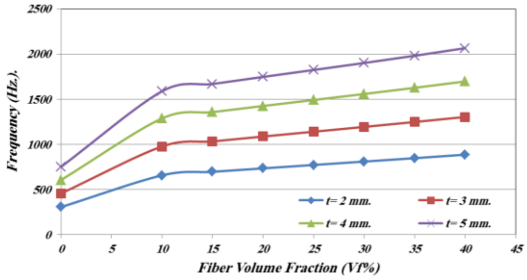

(e)L=0.2 m and W=0.2 m .

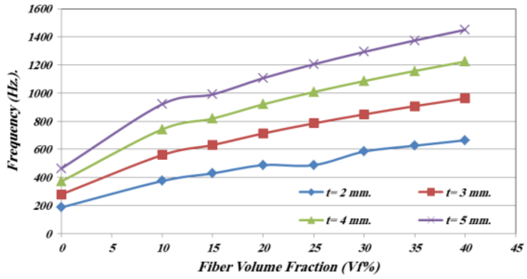

(f) L=0.2 m and W=0.3 m .

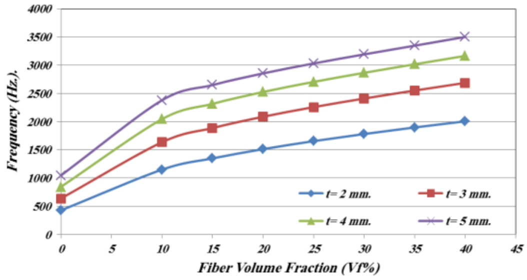

(g) L=0.3 m and W=0.1 m .

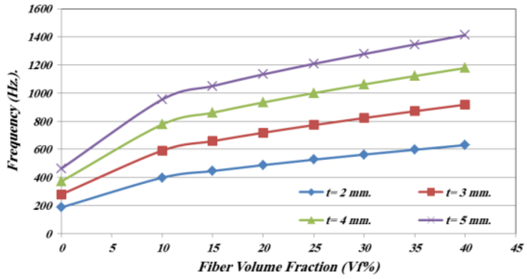

(h) L=0.3 m and W=0.2 m .

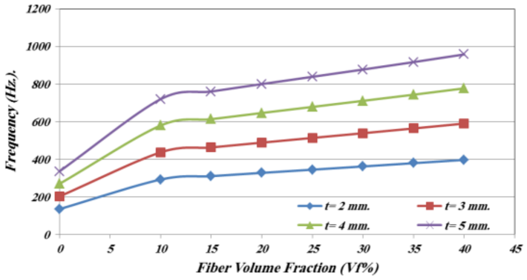

(i) L=0.3 m and W=0.3 m .

Fig. 9. Comparison Between the Forth Natural Frequencies for Different Plate Thickness Due to Change in Fibre Volume Fraction for Different Dimensions of Plate Using the Second Model.

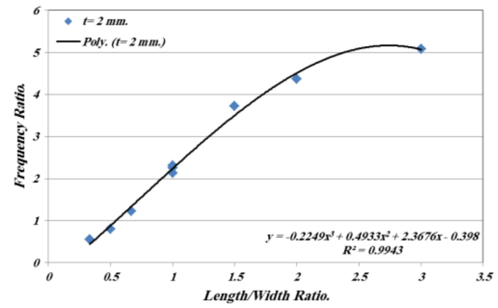

(a) t=2 mm.

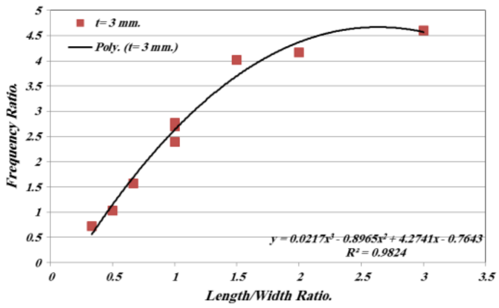

(b) t=3 mm.

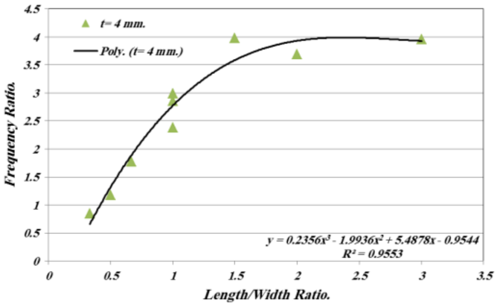

(c) t=4 mm.

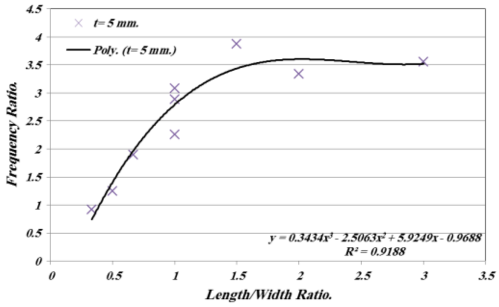

(d) t=5 mm.

Fig. 10. Comparison Between the First Natural Frequency Ratio (Frequency calculating by Second Model /Frequency calculating by First Model) Due to Change Aspect Ratio of Plate (Length/ Width) for Different Plate Thickness.

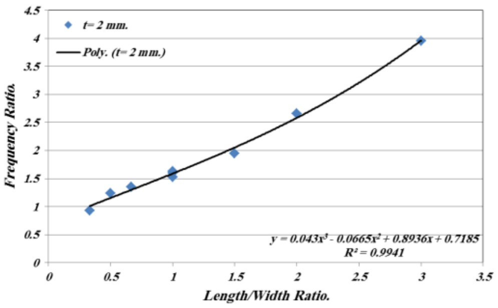

(a) t=2 mm.

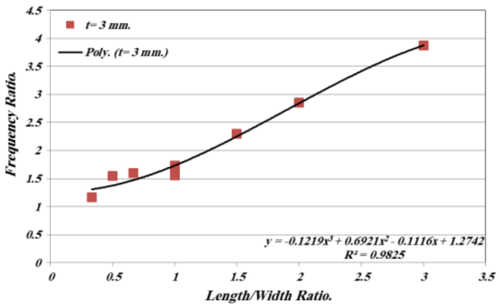

(b) t=3 mm.

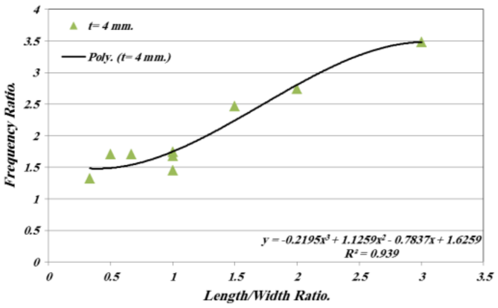

(c) t=4 mm.

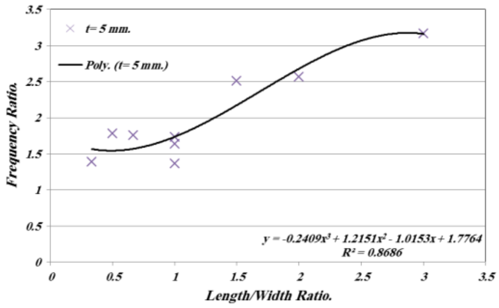

(d) t=5 mm.

Fig. 11. Comparison Between the Second Natural Frequency Ratio (Frequency calculating by Second Model /Frequency calculating by First Model) Due to Change Aspect Ratio of Plate (Length/ Width) for Different Plate Thickness.

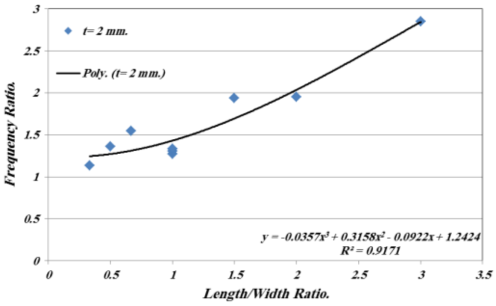

(a) t=2 mm.

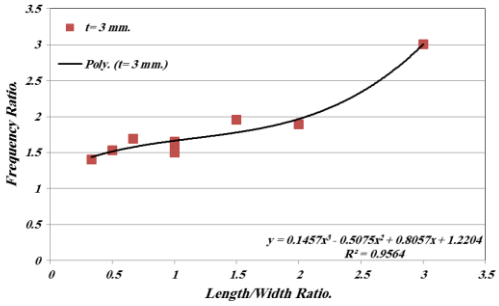

(b) t=3 mm.

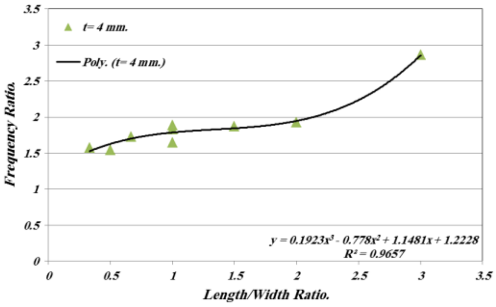

(c) t=4 mm.

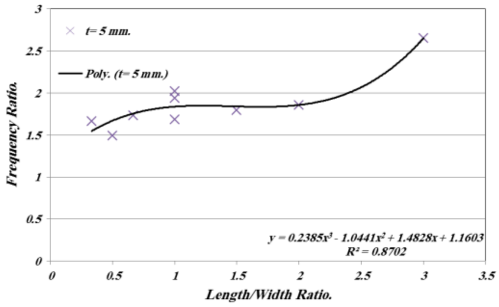

(d) t=5 mm.

Fig. 12. Comparison Between the Third Natural Frequency Ratio (Frequency calculating by Second Model /Frequency calculating by First Model) Due to Change Aspect Ratio of Plate (Length/ Width) for Different Plate Thickness.

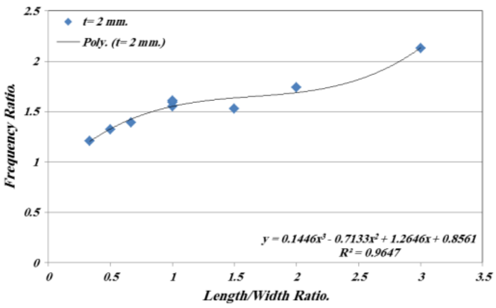

(a) t=2 mm.

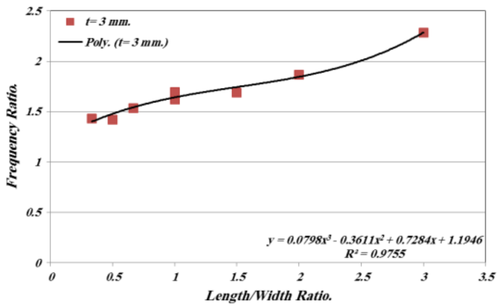

(b) t=3 mm.

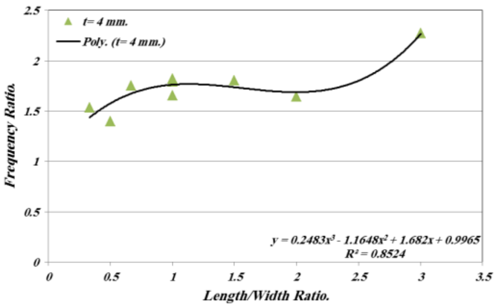

(c) t=4 mm.

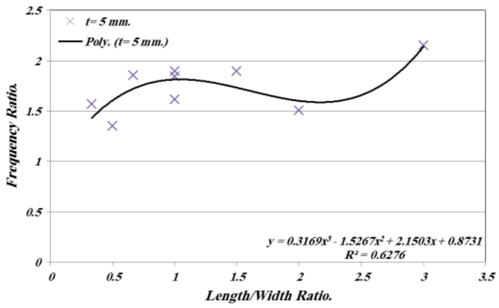

(d) t=5 mm.

Fig. 13. Comparison Between the Fourth Natural Frequency Ratio (Frequency calculating by Second Model /Frequency calculating by First Model) Due to Change Aspect Ratio of Plate (Length/ Width) for Different Plate Thickness.

Table 4. Natural Frequency Ratio (Frequency Second Model /Frequency First Model) with Ratio of Plate (Length/ Width) for Different Plate Thickness.

No $\boldsymbol{\beta = \frac{f_2}{f_1}}$	Thickness	Natural Frequency Ratio function of Plate Ratio
1	$t = 2mm$	$\beta = -0.2249\alpha^3 + 0.4933\alpha^2 + 2.3676\alpha - 0.398$
	$t = 3mm$	$\beta = 0.0217\alpha^3 - 0.8965\alpha^2 + 4.2741\alpha - 0.7643$
	$t = 4mm$	$\beta = 0.2356\alpha^3 - 1.9936\alpha^2 + 5.4878\alpha - 0.9544$
	$t = 5mm$	$\beta = 0.3434\alpha^3 - 2.5063\alpha^2 + 5.9249\alpha - 0.9688$
2	$t = 2mm$	$\beta = 0.043\alpha^3 - 0.0665\alpha^2 + 0.8936\alpha + 0.7185$
	$t = 3mm$	$\beta = -0.1219\alpha^3 + 0.6921\alpha^2 - 0.1116\alpha + 1.2742$
	$t = 4mm$	$\beta = -0.2195\alpha^3 + 1.1259\alpha^2 - 0.7837\alpha + 1.6259$
	$t = 5mm$	$\beta = -0.2409\alpha^3 + 1.2151\alpha^2 - 1.0153\alpha + 1.7764$
3	$t = 2mm$	$\beta = -0.0357\alpha^3 + 0.3158\alpha^2 - 0.0922\alpha + 1.2424$
	$t = 3mm$	$\beta = 0.1457\alpha^3 - 0.5075\alpha^2 + 0.8057\alpha + 1.2204$
	$t = 4mm$	$\beta = 0.1923\alpha^3 - 0.778\alpha^2 + 1.1481\alpha + 1.2228$
	$t = 5mm$	$\beta = 0.2385\alpha^3 - 1.0441\alpha^2 + 1.4828\alpha + 1.1603$
4	$t = 2mm$	$\beta = 0.1446\alpha^3 - 0.7133\alpha^2 + 1.2646\alpha + 0.8561$
	$t = 3mm$	$\beta = 0.0798\alpha^3 - 0.3611\alpha^2 + 0.7284\alpha + 1.1946$
	$t = 4mm$	$\beta = 0.2483\alpha^3 - 1.1648\alpha^2 + 1.682\alpha + 0.9965$
	$t = 5mm$	$\beta = 0.3169\alpha^3 - 1.5267\alpha^2 + 2.1503\alpha + 0.8731$

7. CONCLUSION

From the conducted results, it has been observed that the natural frequency increases when the value of fiber volume fraction increases. The increasing in the fiber volume fraction leads to increase in the modules of elasticity of composite plate.

It has been found that when the plate is fixed from all the sides, the highest natural frequency is achieved compared to other considered boundary conditions.

Furthermore, the numerical equations that derived from these relations as a function of the (length/width) ratio was used to investigate the natural frequencies for longitudinal composite plates.

8. REFERENCES

Akavci S. S. Buckling and free vibration analysis of symmetric and antisymmetric laminated composite plates on an elastic foundation. Jour.of Reinf, Plastic & Composites; 2007.

Alexander J., Kumar H. A., Augustine B. “Frequency Response of Composite Laminates at Various Boundary Conditions”. International Journal of Engineering Science Invention (IJESI), 2012, ISSN (Online): 2319 – 6734, ISSN (Print): 2319 – 6726 www.ijesi.org ǁ PP.11-15.

Andrzej Teter, Jarosław Gawryluk. Experimental modal analysis of a rotor with active composite blades. Composite Structures 2016;153:451–467.

Edward F. Crawley. The Natural Modes of Graphite/Epoxy Cantilever Plates and Shells. Journal of Composite Materials 1979;13:195.

Gay D., Hoa S. V., Tsai S. W. Composite Materials Design and Applications. Book, CRC Press LLC; 2003.

Han W. and Petyt M.. Linear vibration analysis of laminated rectangular plates using the hierarchical finite element method—I, Free vibration analysis. Computers &amp Structures 1996;61:705-712.

Hsu, M.-H. Vibration analysis of isotropic and orthotropic plates with mixed boundary conditions. Tamkang Journal of Science and Engineering 2003;6:217-226.

Latheswary S., Valsajian K. V., Rao Y V K S. Free vibration analysis of laminated plates using higher-order shear deformation theory. IE(I) Jornal-AS; 2004.

Lopatin A.V., Morozov E.V. Fundamental frequency and design of the CFCF composite sandwich plate. Composite Structures 2011;93: 983–991

Leissa A. W.. The free vibration of rectangular plates. Journal of Sound and Vibration 1973;31:257-293.

Pandit, M. K., Haldar, S., Mukhopadhyay, M.. Free vibration analysis of laminated composite rectangular plate using finite element method. Jour. Of Reinforced Plastic & composites; 2007.

Parsuram Nayak. Vibration Analysis of Woven Fiber Glass/Epoxy Composite Plates. M.Sc. Thesis, Department of Civil Engineering, National Institute of Technology Rourkela, Orissa, India; 2008.

Reddy J. N.. Free vibration of ant symmetric, angle-ply laminated plates including transverse shear deformation by the finite element method. Journal of Sound and Vibration 1979;66: 565-576.

Sang Wook Kang, Sang-Hyun Kim. Vibration analysis of simply supported rectangular plates with unidirectional, arbitrarily varying thickness. Jour. Of Sound & Vibr 2008;312:551-562.

Sharma. A. K., Mittal. N.D. Review on stress and vibration analysis of composite plate. Journal Applied Sci 2010;10(23):3156-3166.
William D. Callister, Jr. and David G. Rethwisch. Materials Science and Engineering An Introduction. John Wiley & Sons, Inc; 2010.